Atmos. Meas. Tech. Discuss., 5, 8435–8468, 2012
www.atmos-meas-tech-discuss.net/5/8435/2012/
doi:10.5194/amtd-5-8435-2012

Atmospheric Measurement Techniques Discussions

Multispectral information for gas and aerosol retrieval from TANSO-FTS instrument

H. Herbin, L. C. Labonnote, and P. Dubuisson

Laboratoire d'Optique Atmosphérique (LOA), UMR8518, CNRS – Université de Lille 1, 59655 Villeneuve d'Ascq cedex, France

Received: 14 November 2012 – Accepted: 15 November 2012
– Published: 26 November 2012

Correspondence to: H. Herbin (herve.herbin@univ-lille1.fr)

Published by Copernicus Publications on behalf of the European Geosciences Union.

Abstract

The Greenhouse gases Observing SATellite (GOSAT) mission and in particular TANSO-FTS instrument has the advantage to measure simultaneously the same field of view in different spectral ranges with a high spectral resolution. These features are promising to improve, not only, gaseous retrieval in clear sky or scattering atmosphere, but also to retrieve aerosol parameters.

Therefore, this paper is dedicated to an Information Content (IC) analysis of potential synergy between thermal infrared, shortwave infrared and visible, in order to obtain a more accurate retrieval of gas and aerosol. The latter is based on Shannon theory and used a sophisticated radiative transfer algorithm developed at "Laboratoire d'Optique Atmosphérique", dealing with multiple scattering. This forward model can be relied to an optimal estimation method, which allows simultaneously retrieving gases profiles and aerosol granulometry and concentration. The analysis of the information provided by the spectral synergy is based on climatology of dust, volcanic ash and biomass burning aerosols. This work was conducted in order to develop a powerful tool that allows retrieving simultaneously not only the gas concentrations but also the aerosol characteristics by selecting the so called "best channels", i.e. the channels that bring most of the information concerning gas and aerosol. The methodology developed in this paper could also be used to define the specifications of future high spectral resolution mission to reach a given accuracy on retrieved parameters.

1 Introduction

Satellite observations of the Earth allow continuous monitoring of the atmosphere from local to global scale. Among them, passive remote sensing instruments, which span a broad frequency range from UV to microwave, provide lots of different information on gases, clouds or aerosols atmospheric composition. Nevertheless, although major efforts have been made from observation and modeling, various atmospheric constituents are, up to now, estimated with a large uncertainty (Forster et al., 2007). Traditionally, instrumental specifications (spectral range, spectral resolution, multiple viewing angles, polarization...) are defined to derive specifically only few parameters. In consequence, the radiative transfer models are developed in order to simulate a specific spectral region and optimized to retrieve only one type of atmospheric parameter. For instance, high resolution infrared sounders such as TES (Beer et al., 2011), IASI (Schlüssel et al., 2005, Clerbaux et al., 2007) or TANSO-FTS Kuze et al., 2009) are currently used for gaseous compounds estimation, while broadband sensors such as MODIS (Remer et al., 2005), and multiple viewing angle and/or polarization instruments such as MISR (Kahn et al., 2005) or PARASOL (Tanré et al., 2011) are more dedicated to aerosols and clouds. Some studies such as Cho and Staelin (2006), Li et al. (2004) or Aires et al. (2011) have demonstrated that the use of simultaneous, but different, observations can improve the accuracy of the retrieved parameters. Nevertheless, the applications remain particularly sparse because using information from different instruments is notoriously difficult (collocation, Field of view size and homogeneity...). Moreover, measurements obtained by the same instrument at different spectral range are very promising but are not really exploited, because such methodologies need to take into account others parameters such as spectral and radiometric band to band calibration and also the development of more complex algorithms which are highly time consuming.

Here, we present the contribution of the multi-spectral measurements for an optimal retrieval of gas and aerosol parameters. In particular, we discuss the interest of using two or more spectral range simultaneously in term of accuracy improvement. This synergetic approach is evaluated from the four spectral ranges of the TANSO-FTS instrument.

The GOSAT mission and its two instruments are briefly described in the Sect. 2. The forward model which allows treating simultaneously high resolution infrared and visible measurements and performed to study gas composition in presence of scattering particles is presented in the Sect. 3. The Sect. 4 gives the theoretical bases

AMTD
5, 8435–8468, 2012

of the Information Content (IC). The IC analysis, which is separated on 3 cases: (1) gaseous profiles in clear sky condition, (2) gaseous columns in presence of an aerosol layer, and (3) simultaneous gas and aerosol retrieval, is detailed in Sect. 5. Finally, the Sect. 6 summarizes our results and presents perspectives on future applications.

2 Instruments description

The Greenhouse gases Observing SATellite (GOSAT), which was launched on 23 January 2009 by JAXA, is designed to monitor the global CO_2 and CH_4 distributions from space. GOSAT was put in a sun-synchronous orbit at 666 km altitude with three-day recurrence, and measurements around 13:00 h local time. It is equipped with two instruments, the Thermal And Near infrared Sensor for carbon Observation-Fourier Transform Spectrometer (TANSO-FTS) and the Cloud and Aerosol Imager (TANSO-CAI). The TANSO-FTS performs high-spectral-resolution measurements (0.2 cm^{-1}, non-apodized) in Thermal InfraRed (TIR) (700–1800 cm^{-1}), Short Wave InfraRed (SWIR) (4800–5200 and 5800–6400 cm^{-1}) and visible (12 900–13 200 cm^{-1}) with an instantaneous field of view of 15.8 mrad, which corresponds to a nadir circular footprint of about 10.5 km. For the SWIR and visible bands, the incident light is recorded as two (P and S) orthogonal polarization components. TANSO-CAI has four narrow bands in the near ultraviolet to near-infrared regions at 0.38, 0.674, 0.87, and 1.6 µm, with spatial resolutions of 0.5, 0.5, 0.5, and 1.5 km, respectively, for nadir pixels.

3 Radiative transfer and forward model

Accurate calculations of the radiances observed by TANSO-FTS are achieved with the high spectral resolution (up to 0.0001 cm^{-1}) code LBLDOM (Dubuisson et al., 1996, 2005) over the thermal and solar spectral regions (0.2–16 µm). Radiances at the top of the atmosphere are calculated by solving the Radiative Transfer Equation (RTE) in a horizontally homogeneous scattering atmosphere, using the Discrete Ordinate Method

AMTD
5, 8435–8468, 2012

(DOM) (Stamnes et al., 1988). Gaseous absorption is calculated with a line-by-line code based on STRANSAC (Scott, 1974) and the HITRAN 2008 database (Rothman et al., 2009). The absorption lines computation includes Lorentz, Doppler and Voigt line-shape as a function of the thermodynamic profile of the atmosphere. Absorption continua (H_2O, CO_2, and N_2) are also included from the MT-CKD parameterization (Clough et al., 2005). The solar irradiances database reported by Kurucz (http://kurucz.harvard.edu/sun/irradiance2008/) is used as the incident solar spectrum. The RTE resolution using DOM approach allows taking into account absorption, emission, Rayleigh and multiple scattering processes for aerosol and gaseous species. Aerosols are defined from their optical parameters: optical thickness, single scattering albedo and phase function. These parameters are obtained from a Mie scattering code assuming spherical particles with a bi-modal and lognormal distribution. Note that concerning clouds, the spherical assumption is still valid for liquid cloud but not for ice clouds. The latter need a code accounting for different particle shapes, and will not be discussed in this paper. Finally, the total intensity of TANSO-FTS spectra are simulated using the Instrumental Line Shapes (ILS) provided for each four bands by the GOSAT user interface gateway (https://data.gosat.nies.go.jp/gateway/gateway/MenuPage/open.do) and no post-apodization is applied, this allows exploiting the full spectral resolution.

The Fig. 1 illustrates the forward model capabilities to simulate the fours bands of TANSO-FTS in clear sky conditions. It shows an example of observed spectrum in Nadir-viewing and the individual contributions of major molecular absorbers on US Standard profiles. Even if this instrument is mainly dedicated to CO_2 and CH_4 measurement, its instrumental qualities (spectral range, spectral resolution and signal to noise ratio) could enable detection of number of other species less absorbing in particular during special events (volcanic eruption, biomass burning, pollution areas...).

AMTD
5, 8435–8468, 2012

4 Theoretical bases on information content

Sensitivity studies are often used to understand the response of individual measurements to a set of parameters (state vector), but to determine the combination of channels best suited for the retrieval, it is important to take into account the measurements and forward model accuracy. The IC theory, first developed by Shannon and Weaver (1949), is well suitable to analyze the properties of an observing system.

The theoretical elements relevant for the present information content analysis are similar to those described by Rodgers (2000). They are only briefly summarized hereafter.

We adopt the definition of Shannon and Weaver (1949) hereinafter referred as Shannon Information Content (SIC). Several studies have recently applied this method, for instance, to analyze the CO_2 vertical column information from multispectral radiance measurements, such as AIRS or IASI (Engelen and stephens, 2004), to analyze information on cloud microphysics from MODIS (L'Ecuyer et al., 2006; Cooper et al., 2006), but also to determine the instrumental specifications of future missions, such as IASI-NG (Herbin and Labonnote, personal communication, 2012).

The SIC is based on a measure of knowledge of an observing system, before and after a measurement is made. The quantity used is analog to the thermodynamic entropy S, define as the number of different internal states of a macroscopic system. Therefore, the information given by a measurement on that system is related to its entropy reduction. Letting P_1 the Probability Distribution Function (PDF) prior to the measurement (this PDF represents the probability of obtaining any state in the retrieval problem), and P_2 the PDF after the measurement is made, the SIC is then defined as:

$$H = S(P_1) - S(P_2) \tag{1}$$

The H parameter quantifies how the addition of the measurements reduces the number of possible states which explain simultaneously our prior knowledge of the system and the measurements made. If we assume that the PDFs follow Gaussian distributions

AMTD
5, 8435–8468, 2012

with variance-covariance matrix S_1 and S_2 respectively, then Rodgers (2000) demonstrated that we can write the SIC as:

$$H = \frac{1}{2}\log_2 \left| S_1 S_2^{-1} \right| \tag{2}$$

In this formulation, and because entropy is defined as the logarithm in base 2 of the total number of state, H provides an information content in bits, which means that after a measurement is made we can potentially distinguish 2^H states in the prior state space volume. Currently, we usually used the Degree Of Freedom for signal (DOFs) which represents the number of independent pieces of information contains in the measurement. The latter can be written as follows:

$$\text{DOFs} = \text{tr}(S_1 S_2^{-1}) \tag{3}$$

In case of an atmosphere divided in discrete layers, the forward radiative transfer equation gives an analytical relationship between the set of observations y (here, the radiances) and the vector of true atmospheric parameters x and is written as:

$$y = \boldsymbol{F}(\boldsymbol{x}) + \boldsymbol{\varepsilon} \tag{4}$$

where $\boldsymbol{F}$ represents the model which allows mapping the state space to the measurement space and $\boldsymbol{\varepsilon}$ the measurements and/or forward model errors vector. Let $\mathbf{S}_a$ and $\mathbf{S}_x$ being the covariance matrix describing our knowledge of the state space prior and posterior to the measurement. In the formalism of Gaussian PDF, the measurements and forward model accuracy can be represented with covariance matrices $\mathbf{S}_m$ and $\mathbf{S}_b$, respectively. The latter describe the error associated with uncertainties on the forward model parameters that are not retrieved. Rodgers (2000) demonstrated that the error variance-covariance matrix describing the posterior state space can be written as:

$$\mathbf{S}_x = (\mathbf{S}_a^{-1} + K^T S_\varepsilon^{-1} K)^{-1} \tag{5}$$

where $\mathbf{S}_\varepsilon = \mathbf{S}_m + \mathbf{S}_b$, and K is the Jacobian of the forward model with respect to the state vector $\boldsymbol{x}$. The coefficient K_{ij} of this matrix $\mathbf{K}$ is given by $K_{ij} = \frac{\partial F_i}{\partial x_j}$.

AMTD
5, 8435–8468, 2012

4.1 Channel selection

Because the computation time required to perform the simulation of the entire GOSAT spectrum is very large, it is fundamental to reduce the number of channels used in the inversion procedure. As emphasis by Rodgers (2000), the SIC framework is very well suited to optimize the selection of channels that carry the greatest amount of information. The procedure first requires to build the so called "information spectrum" which is the information content attach to each individual measurement with respect to the prior knowledge of the state vector. The channel that carries the largest amount of information is then selected and its information is removed from the remaining channels to get a new "information content" spectrum. This is done by adjusting the posterior covariance matrix to account for the information provided by the selected channel. This process is repeated and channels are selected until the information provided by the remaining channels fall below the level of measurement noise, or until the specification of the mission is reached. The details of the theoretical elements of this procedure and examples are provided in the reference (L'Ecuyer et al., 2006).

4.2 Error description

Accurate characterization of the error covariance matrices is central to the problem of calculating SIC as well as for global retrievals based on variational method.

4.2.1 Prior covariance matrix

In practice $\mathbf{S}_a$ is easier to define because it merely represents our knowledge of the system before the measurements is made. It could be evaluated from climatology or in-situ data. Even if prior information could be very valuable to reduce the volume of the prior state vector, we assume in this theoretical study a very small prior knowledge. This choice is justified by the fact that this study focuses on the information content to perform retrievals in a general case and thus highlight information coming from the

Discussion Paper | Discussion Paper | Discussion Paper | Discussion Paper |

AMTD

5, 8435–8468, 2012

Multispectral information for gas and aerosol retrieval

H. Herbin et al.

measurement. Therefore, we will always assume $\mathbf{S}_a$ as a diagonal matrix with an error (P_{error}) of 100 % on the prior state vector $\boldsymbol{x}_a$ with:

$$\boldsymbol{\sigma}_{a,i} = x_{a,i} \cdot \frac{P_{\text{error}}}{100} \quad \text{and} \quad \mathbf{S}_{a,ii} = \boldsymbol{\sigma}^2_{a,i} \tag{6}$$

where $\mathbf{S}_{a,i}$ stand for the standard deviation in the Gaussian statistics formalism. The subscript i represent the i-th parameter of the state vector.

4.2.2 Measurement covariance matrix

In order to compute the measurement covariance matrix, one needs to know the instrument performance or accuracy. By instrument performance one can understand the radiometric calibration (which could be a bias) and radiometric noise, usually given as a Signal to Noise Ratio (SNR). This covariance matrix is assumed diagonal (each individual measurement is independent) and can be computed as follow:

$$\mathbf{S}_{m,ii} = \sigma^2_{m,i} \tag{7}$$

where $\mathbf{S}_{m,i}$ is the standard deviation of the i-th measurement of the measurement vector, representing the noise equivalent spectral radiance. Its value is constant for each spectral band and given for a signal to noise ratio of about 300 (Kuze et al., 2009).

4.2.3 Forward model covariance matrix

Evaluation of the forward model error or accuracy is the most difficult part of the error description. Indeed, it consists in both, the model precision (for example 1-D approximation, Lambertian surface,...) as well as error due to the non retrieve parameters (x_b) used in the forward model (e.g. temperature profile, ground emissivity,...). Because horizontal variability of gas and aerosol are small enough on a GOSAT pixel size, and

AMTD
5, 8435–8468, 2012

because it is beyond the scope of this paper to explore 3-D effects due to horizontal sub-pixel heterogeneity, we choose to neglect it in this study. Thus, only effects of non-retrieve parameters uncertainties are explored here.

The most important variables when dealing with infrared measurements such as GOSAT Band 4 are the temperature profile and surface temperature. We assume a realistic uncertainty of 1 K on each layer of the temperature profile as well as on surface temperature, and the contribution to the forward model covariance matrix can be found as:

$$\sigma_{b,T_j,i} = \frac{\partial F_i}{\partial T_j}\Delta T \tag{8}$$

where $\Delta T = 1$ K and j stand for the j-th level.

The surface emissivity ($\boldsymbol{\varepsilon}$) is fixed to 1, 0.98, 0.98 and 0.95 for Bands 4, 3, 2 and 1 respectively with an uncertainty (p_e) of 5 %.

$$\boldsymbol{\sigma}_{b,\varepsilon,i} = \frac{\partial F_i}{\partial \boldsymbol{\varepsilon}}\Delta\boldsymbol{\varepsilon} \quad \text{with} \quad \Delta\boldsymbol{\varepsilon} = \frac{p_\varepsilon}{100}\boldsymbol{\varepsilon} \tag{9}$$

For the same reason as explained in the Sect. 4.2.1, we also assume a little knowledge on the interfering molecules concentration with an uncertainty (P_{Cmol}) of 100 %.

$$\sigma_{b,c_{\text{mol}^k},i} = \frac{\partial F_i}{\partial c_{\text{mol}^k}}\Delta c_{\text{mol}^k} \quad \text{with} \quad \Delta c_{\text{mol}^k} = \frac{p_{\text{Cmol}}}{100}c_{\text{mol}^k} \tag{10}$$

where C^k_{mol} represents the concentration of the k-th interfering molecule.

Finally, the total forward model covariance matrix ($\mathbf{S}_b$, assumed diagonal) is given by summing all this error contribution for each diagonal elements ($S_{b,ii}$):

$$S_{b,ii} = \sum_{j=1}^{\text{nlevel}} \sigma^2_{b,T_j,i} + \sum_{k=1}^{\text{nmolecules}} \sigma^2_{b,c_{\text{mol}^k},i} + \sigma^2_{b,\varepsilon,i} \tag{11}$$

AMTD
5, 8435–8468, 2012

5 TANSO-FTS multispectral information

5.1 SIC apply to gaseous species profiles in clear atmosphere

High spectral resolution infrared instruments, such as AIRS (Strow et al., 2003), TES or IASI which span roughly the Band 4 (TIR) of TANSO-FTS, have been mainly used to retrieve CO_2 (Maddy et al., 2008; Crevoisier et al., 2009; Kulavik et al., 2010), CH_4 (Xiong et al., 2008; Razavi et al., 2009; Worden et al., 2012) and H_2O (Gao et al., 2006; Worden et al., 2006; Herbin et al., 2009) atmospheric columns concentrations. Moreover, recent works have been conducted to retrieve CH_4 and CO_2 columns concentrations from Bands 2 and 3 (SWIR) of TANSO-FTS (Yoshida et al., 2011). In order to quantify the benefit of multispectral synergy, it is essential to perform, first, an information content analysis of such observing system on CO_2, CH_4 and H_2O profiles in clear sky condition. For that, we have used an a priori state vector $\boldsymbol{x}_a$ based on US Standard profile discretized on 11 vertical levels, extending from the ground to 20 km.

The Fig. 2 shows the vertical DOFs for the three gaseous species by considering the Bands 2, 3 and 4 alone and all the bands together. Concerning H_2O, the lines corresponding to the DOFs given by the use of all the bands (solid lines) and Band 4 alone (dash lines) are practically superposed, which means that the information mainly comes from Band 4. Nevertheless although less sensitive, Band 2 and Band 3 can be interesting together to enhance the information in the lower atmosphere. Regarding CO_2, the maximum information is provided by Bands 3 and 4 but the combined use of these two bands is more favorable, especially under 7 km. For CH_4, we can notice that the DOFs given by the use of Band 4 alone and all the bands together are very similar and the difference is not really distinguishable.

All these remarks are confirmed by the Fig. 3, which gathers the corresponding total error profiles (given by the square root of the diagonal elements of $\mathbf{S}_x$) as well as the contribution of the a-priori $\mathbf{S}_a$), non-retrieve parameters (forward model errors, $\mathbf{S}_b$) and measurements errors ($\mathbf{S}_m$). Thus, the Fig. 3 allows a more detailed analysis of the retrieval capacity. As a general trend, we can notice that for the three species, the

AMTD
5, 8435–8468, 2012

simultaneous use of all the bands instead of Band 4 alone, reduce systematically the total errors in the lower part of the atmosphere up to 4 km and mostly between 0 and 2 km. This is consistent with the fact that in case of clear sky, Band 4 corresponds to the radiation emitted by the ground, while Bands 1, 2 and 3 are the solar radiances reflected on the Earth's surface.

As already seen previously, most of the information is related to H_2O which should be retrieved between 0 and 10 km with a vertical resolution of at least 2 km and an associated error of about 4 %. This total error is only limited by measurement uncertainty pointing out the high sensitivity of such measurements to H_2O concentration, especially for Band 4. We can notice a different behavior above 12 Km where the error is mainly governed by the a priori uncertainty, which can be explained by the lost of sensitivity at this altitude. Indeed, it is important to note that the total errors are regularly governed by the a priori error $\mathbf{S}_a$. This is due to the fact that we deliberately chose to set a large uncertainty on the prior state vector $\boldsymbol{x}_a$ (100 % uncertainty) which deteriorates dramatically the total error when the measurement sensitivity decreases (cf. Eq. 5). The Figs. 2 and 3 highlight the difficulty to retrieve a CH_4 profile from such measurements without a priori constrain. It is merely impossible to obtain better than one tropospheric column (e.g. between 2 and 12 km), and the use of Band 4 alone seems to be sufficient. Concerning CO_2, the Band 4 remains the most favorable and allows obtaining two levels of information, which could be divided in two partial columns between 0–6 km and 6–12 km.

Thus, the analysis of Figs. 2 and 3 confirms that the Band 4 is the most suitable for obtaining gaseous vertical profiles in clear sky condition. However, for CO_2 and CH_4, the SWIR Bands have the advantage of having low measurement and non-retrieved parameters errors. The latter can be explained by weak temperature dependence and less interference from other molecules than Band 4 (see for instance Band 2 of the Fig. 1), and justify the instrumental specifications of TANSO-FTS as described in Kuze et al. (2009). So, Bands 2 and 3, although less sensitive, are commonly used for total

AMTD
5, 8435–8468, 2012

columns retrievals, but, the lack of sensitivity requires perfectly constrain the inversion by an adapted $\mathbf{S}_a$ matrix (Yoshida et al., 2011).

Finally, it is important to remember that this information contents analysis is theoretical. Indeed, in the context of an inversion procedure it is almost impossible to use the 12 000 channels altogether. Firstly because it would be very difficult to properly establish an accurate state vector $\boldsymbol{x}_a$ and a variance-covariance matrix $\mathbf{S}_a$ for all the variables, or the non-retrieved parameters error $\mathbf{S}_b$ would be very large, and secondly because the amount of channels to be processed would require a huge computing time. Thus, it appears necessary to make a channels selection which achieve the best compromise between accuracy on one side and the complexity and computation time on the other side. Therefore, Figs. 4 and 5 show the DOFs and errors respectively, for two different cases: (1) we selected, thanks to the method describe in Sect. 4.1, the first hundred "best" channels and (2) the first thousand "best" channels. These quantities correspond to realistic values of the number of channels used for gaseous concentration retrievals in clear sky conditions. In order to understand the usefulness of the spectral synergy, this selection was made either from all the channels available or from the channels of Band 4 alone. A direct comparison between Figs. 2 and 3 with Figs. 4 and 5 reveal that the information carrying from case 2 (first thousand best channels) is very similar to the one using all the available channels. Moreover, when using only 100 channels we can remark a significant lost of accuracy over the entire vertical profile for CO_2 and CH_4, whereas it remains almost identical for water vapor up to 7 km. It is also interesting to mention the significant increase of the errors between case 2 and case 1 especially in the first two kilometers. More generally, this study confirm the interest of the spectral synergy when performing a channels selection over all the bands (from infrared to visible), it also shows that using the first thousand "best" channels do not degrade significantly the information on the vertical concentrations of the three studied gas.

AMTD
5, 8435–8468, 2012

5.2 SIC apply to gaseous species total columns in scattering atmosphere

It is notoriously known that the flux in SWIR includes surface reflection and multiple scattering of aerosol, else clear sky observations are only a small part of the entire set of measurements (Eguchi and Yokota, 2008). Obviously, the gas concentrations retrieval in the presence of an aerosol layer without taking it into account in the forward model, either the calculation cannot converge, either the results will be obtain with a very large error or bias. This section is therefore dedicated to study the effect of the presence of an aerosols layer on the gas column information content. The objective is to understand the behavior of the information, when we take into account an aerosol layer in the forward model, but without retrieving it. This configuration corresponds to the situation where one wants to use aerosol information from ancillary data (e.g. retrieval from other instruments mainly dedicated to aerosol study). In order to reflect the nature diversity in terms of atmospheric aerosols, we used the general granulometric properties for three different aerosol types. These properties (number of particles C (in part m^{-3}), mean radius r (in µm) and standard deviation logarithm ln (σ)) come from Dubovik et al. (2002) for dust and biomass burning, and from Tanré et al. (2012) for volcanic ash. All this granulometric properties are summarized in Table 1. For each aerosol type, we have fixed one layer with a thickness of 2 km, located between 3–5 km for biomass burning, 5–7 km for dust and 7–9 km for volcanic ash. The radiance spectra for each TANSO-FTS bands, illustrated on Fig. 6, are calculated from our forward model with refractive indices from Sutherland and Khanna (1991) for biomass particles, Pollack et al. (1973) for ash and Volz (1973) for sand dust, assuming a bi-modal lognormal distribution.

In order to take into account their influence on the information and errors about the gas column, we have to specify the uncertainty of each aerosol parameter needed in the forward model computation (e.g. to compute the matrix $\mathbf{S}_b$). The aerosol parameters C, r, ln (σ)) and refractive indices are supposed to be known with an uncertainty of 100 %. An aerosol layer height error of 1 km is also assumed and the knowledge of the others atmospheric parameters are identical to the one of Sect. 4.2. Figure 7 shows the DOFs and theoretical errors on the column concentration of H_2O, CO_2 and CH_4 for the Bands 2, 3 and 4 separately and all the bands together, as a function of aerosol optical depth (τ) from 0.05 to 3 for volcanic ash and biomass burning particles, and from 0.05 to 1.5 for dust. In order to facilitate the comparison with dedicated instruments, the optical thickness values are taken from the aerosol model extrapolation at 1020 nm for dust, 440 nm for biomass particles (Dubovik et al., 2002) and 865 nm for volcanic ash (Tanré et al., 2012). Moreover, the space agencies defined the mission specifications where each gas column had to be retrieved within a given error. For instance, for the GOSAT mission, the latter is estimated to 1 % for CO_2 and 2 % for CH_4. Therefore, the discussion that follows is organized around the ability of a given observing system to reach the specification mission with or without channels selection.

The general trend is that the information (in terms of DOFs) strongly depends of the aerosol optical thickness whatever the nature of the aerosol for an observing system composed of Bands 2 or 3 alone. This trend almost vanishes for an observing system that would use Band 4 alone or all the bands together. Moreover, the corresponding lines of the latter (red and black solid line respectively) are almost systematically superposed which means that most of the information comes from Band 4. Therefore, an important conclusion of this study is that even with the presence of a scattering layer in the atmospheric column, Band 4 seems to carry enough information to retrieve gas column properties, whereas Band 2 and 3 seems to provide only partial information which strongly depends of the aerosol optical depth and type.

More specifically, we can see that the DOFs decrease when the aerosol optical depth increase, except for ash when $\tau \geq 0.5$. The water vapour column concentration is well retrieved with a very weak error when Band 4 belongs to the observing system, even if we use only the first thousand “best” channels (see Sect. 4.1), and whatever the aerosol type and optical depth. In contrast, CO_2 and CH_4 columns retrieval appears more difficult and is subject to larger errors (> 2 %) due to the presence of an aerosol layer. For instance, if the aerosol layer is an Ash plume, it seems not possible to reach

AMTD
5, 8435–8468, 2012

the mission specifications for CO_2 and CH_4 even by using all the information from all the bands together (i.e. 12 000 channels). This is not the case in the presence of a Biomass or a Dust layer, pointing out the different behavior with the aerosol type. Another important result is that these mission specifications are reached for CO_2 and CH_4 when the channels selection is done with an observing system that would used all the band together, which is not the case when using Band 4 alone even with low optical thickness ($\tau \leq 0.5$). These results reveal the importance of a spectral synergy in the presence of a scattering layer underneath to get accurate retrieval of CO_2 and CH_4 gas column concentration. Thus, it appears that the information provided by Band 2 and 3 in scattering atmosphere is more important than in cases of clear sky condition, further justifying the use of multispectral synergy for the gaseous columns retrieval in such atmospheric configuration.

Finally, it may be noted that whatever the particles, the CH_4 and CO_2 errors for small optical thicknesses can be compared to Yoshida et al. (2011).

5.3 SIC for simultaneous retrieval of gas and aerosol parameters

In this section, we have treated aerosol as retrieved parameters. First, in order to quantify their impact to the gas columns retrieval, and second to evaluate the available information on the aerosol layer. Here, we use three state vectors corresponding to the most common aerosol observations, that is to say an optical thickness $\tau_{(865\,\mathrm{nm})} = 2.35$ for the ash (Tanré et al., 2012), $\tau_{(440\,\mathrm{nm})} = 0.75$ for biomass particles and $\tau_{(1020\,\mathrm{nm})} = 0.25$ for the dust (Dubovik et al., 2002). The IC including aerosol parameters shows (see Table 2) that including aerosols parameters in the inversed state vector reduces slightly but systematically the uncertainty on the retrieved gaseous columns. In particular, the inversion parameters in presence of biomass particles and dust allows, contrary to Sect. 5.2, achieving the mission specifications for CO_2 and CH_4. Before performing an inversion process for gas and aerosol parameters, it is necessary to know the sensitivity of the measurement to the new state vector. Thus, Fig. 8 shows the DOFs and associated errors for each parameter: that is to say H_2O, CO_2, CH_4 total columns (in

%) and aerosol parameters (number of particles C, mean radius r, and standard deviation σ) indexed c and f, for coarse and fine mode respectively. It may be noticed that in all cases the information is significantly improved compared to the a priori used in the previous section (100 %). For instance, the three volcanic ash parameters of the coarse mode can be determined with an error less than 20 %. Concerning the dust and biomass, the uncertainty is larger, but the sensitivity is important for both modes, even considering an uncertainty of 100 % for the refractive indices.

However, as mentioned above, it appears difficult to exploit all channels in the case of an inversion process. Thus, a selection of 2250 channels, roughly equivalent to the amount used by (Yoshida et al., 2011), here corresponding to approximately 82 % of the total information was performed. We can see in Table 3 that the amount of selected channels from Bands 2 and 3, which are those used by the NIES for the CO_2 and CH_4 operational products, is less than 30 % in presence of ash and biomass particles and about 5 % for dust. This shows that the spectral distribution of the channels selection is highly dependent of the particle type, but also the simultaneous use of Bands 1 and 4 is essential for an accurate inversion of the gases and aerosols parameters. This fully justifies quantitatively the advantages of using the multispectral synergy to improve the IC and therefore the retrievals of tropospheric components.

6 Summary and conclusion

To summarize, the first part demonstrates that in case of clear sky condition and given the instrumental characteristics of TANSO-FTS instrument, we can retrieve between 1 and 2 columns for CH_4, 2 columns for CO_2 and at least 6 columns for H_2O from ground to 20 km, with a good accuracy, with a reduced selection of channels ($\leq$ 1000) mainly from Band 4. The SWIR bands allow the tropospheric columns retrieval, but using an appropriate constraint of the a priori model.

Then, in the presence of aerosols, otherwise assumed to be known, it is possible to obtain H_2O, CO_2 and CH_4 tropospheric columns. However, in this case, the mission specifications are either unachievable (case of ash) or require the use of TIR and SWIR bands simultaneously. Moreover, the need to perform a channels selection for the inversion process restrict the using of this method, which then depends on the nature and altitude of the aerosol layer.

Finally, the retrieval of gas and aerosol parameters simultaneously has the advantage to improve information on the gas columns but also to better characterize the aerosol parameters. This can be done efficiently only by using simultaneously 2 or 3 spectral bands, demonstrating the interest of multispectral synergy for this kind of inversion methodology.

This paper is dedicated to simulated spectra study; in consequence, a future work will exploit real measurements from TANSO-FTS on case studies. In addition, from theoretical point of view, it would be interesting to study also the polarization contribution of the SWIR bands.

Acknowledgements. The authors acknowledge B. Bonnel for his advices on Mie scattering algorithm and F. Ducos for his computing help. This work was supported by the French Space Agency, Centre National d'Etudes Spatiales (CNES), project "GOSAT-TOSCA".

INSU
Institut national des sciences de l'Univers

The publication of this article is financed by CNRS-INSU.

References

Aires, F., Paul, M., Prigent, C., Rommen, B., and Bouvet, M.: Measure and exploitation of multisensor and multiwavelength synergy for remote sensing: 2. Application to the retrieval of atmospheric temperature and water vapor from MetOp, Geophys. Res., 116, D02302, doi:10.1029/2010JD014702, 2011.

Beer, R., Glavich, T. A., and Rider, D. M.: Tropospheric emission spectrometer for the Earth Observing System's Aura Satellite, Appl. Optics, 40, 2356–2367, 2001.

Cho, C. and Staelin, D. H.: Cloud clearing of Atmospheric Infrared Sounder hyper-spectral infrared radiances using stochastic methods, J. Geophys. Res., 111, D09S18, doi:10.1029/2005JD006013, 2006.

Clerbaux, C., Hadji-Lazaro, J., Turquety, S., George, M., Coheur, P.-F., Hurtmans, D., Wespes, C., Herbin, H., Blumstein, D., Tournier, B., and Phulpin, T.: The IASI/MetOp mission: first observations and highlight of its potential contribution to the GMES Earth observation component, Space Res. Today, 168, 19–24, 2007.

Clough, S. A., Shephard, M. W., Mlawer, E. J., Delamere, J. S., Iacono, M. J., Cady-Pereira, K., Boukabara, S., and Brown, P. D.: Atmospheric radiative transfer modeling: a summary of the AER codes, J. Quant. Spectrosc. Ra., 91, 233–244, 2005.

Cooper, S., L'Ecuyer, T., Gabriel, P., Baran, K. A. J., and Stephens, G.: Objective assessment of the information content of visible and infrared radiance measurements for cloud microphysical property retrievals over the global oceans, Part 2: Ice clouds, J. Appl. Meteorol., 45, 42–62, 2006.

Crevoisier, C., Chédin, A., Matsueda, H., Machida, T., Armante, R., and Scott, N. A.: First year of upper tropospheric integrated content of CO_2 from IASI hyperspectral infrared observations, Atmos. Chem. Phys., 9, 4797–4810, doi:10.5194/acp-9-4797-2009, 2009.

Dubovik, O., Holben, B., Eck, T. F., Smirnov, A. Y., Kaufman, J., King, M. D., Tanré, D., and Slutsker, I.: Variability of absorption and optical properties of key aerosol types observed in worldwide locations, J. Atmos. Sc., 59, 590–608, 2002.

Dubuisson, P., Buriez, J. C., and Fouquart, Y.: High spectral resolution solar radiative transfer in absorbing and scattering media: Application to the satellite simulation, J. Quant. Spectrosc. Ra., 55, 103–126, 1996.

Dubuisson, P., Giraud, V., Chomette, O., Chepfer, H., and Pelon, J.: Fast radiative transfer modeling for infrared imaging radiometry, J. Quant. Spectrosc. Ra., 95, 201–220, 2005.

Eguchi, N. and Yokota, T.: Investigation of clear-sky occurrence rate estimated from CALIOP and MODIS observations, Geophys. Res. Lett., 35, L23816, doi:10.1029/2008GL035897, 2008.

Engelen, R. J. and Stephens, G. L.: Information Content of Infrared Satellite Sounding Measurements with Respect to CO_2, J. Appl. Meteor., 43, 373–378, 2004.

Forster, P., Ramaswamy, V., Artaxo, P., Berntsen, T., Betts, R., Fahey, D., Haywood, J., Lean, J., Lowe, D., Myhre, G., Nganga, J., Prinn, R., Raga, G., Schulz, M., and Dorland, R. V.: Changes in atmospheric constituents and in radiative forcing, in Climate Change 2007, the Physical Science Basis, Contribution of Working Group I. to the Fourth Assessment Report of the Intergovernmental Panel on Climate Change, Cambridge U, Press, 2007.

Gao, W., Zhao, F., and Gai, C.: Validation of AIRS retrieval temperature and moisture products and their application in numerical models, Acta Meteorol. Sin., 64, 271–280, 2006.

Herbin, H. and C.-Labonnote, L.: Instrumental specifications of the future instrument IASI-NG: Information content analysis of Water vapour, private communication of the MENINGE (CNES) group, 2011.

Herbin, H., Hurtmans, D., Clerbaux, C., Clarisse, L., and Coheur, P.-F.: $H_2^{16}O$ and HDO measurements with IASI/MetOp, Atmos. Chem. Phys., 9, 9433–9447, doi:10.5194/acp-9-9433-2009, 2009.

Herman, M., Deuzé, J., Marchand, A., Roger, B., and Lallart, P.: Aerosol remote sensing from POLDER/ADEOS over the ocean: improved retrieval using a nonspherical particle model, J. Geophys. Res., 110, D10S02, doi:10.1029/2004JD004798, 2005.

Kahn, R., Gaitley, B., Martonchik, J., Diner, D., Crean, K., and Holben, B.: Multiangle imaging spectroradiometer (MISR) global aerosol optical depth validation based on 2 years of coincident aerosol robotic network (AERONET) observations, J. Geophys. Res., 110, D10S04, doi:10.1029/2004JD004798, 2005.

Kulawik, S. S., Jones, D. B. A., Nassar, R., Irion, F. W., Worden, J. R., Bowman, K. W., Machida, T., Matsueda, H., Sawa, Y., Biraud, S. C., Fischer, M. L., and Jacobson, A. R.: Characterization of Tropospheric Emission Spectrometer (TES) CO_2 for carbon cycle science, Atmos. Chem. Phys., 10, 5601–5623, doi:10.5194/acp-10-5601-2010, 2010.

Kuze, A., Suto, H., Nakajima, M., and Hamazaki, T.: Thermal and near infrared sensor for carbon observation Fourier-transform spectrometer on the Greenhouse Gases Observing Satellite for greenhouse gases monitoring, Appl. Optics, 48, 6716–6733, 2009.

AMTD

5, 8435–8468, 2012

L'Ecuyer, T. S., Gabriel, P., Leesman, K., Cooper, S. J., and Stephens, G. L.: Objective assessment of the information content of visible and infrared radiance measurements for cloud microphysical property retrievals over the global oceans, Part I: Liquid clouds, J. Appl. Meteor. Climatol, 45, 20–41, 2006.
Li, J., Menzel, W. P., Zhang, W., Sun, F., Schmit, T. J., Gurka, J. J., and Weisz, E.: Synergistic use of MODIS and AIRS in a variational retrieval of cloud parameters, J. Appl. Meteorol., 43, 1619–1634, 2004.
Maddy, E. S., Barnet, C. D., Goldberg, M., Sweeney, C., and Liu, X.: CO_2 retrievals from the Atmospheric Infrared Sounder: Methodology and validation, J. Geophys. Res., 113, D11301, doi:10.1029/2007JD009402, 2008.
Pollack, J., Toon, O., and Khare, B.: Optical properties of some terrestrial rocks and glasses, Icarus 19, 372–389, 1973.
Razavi, A., Clerbaux, C., Wespes, C., Clarisse, L., Hurtmans, D., Payan, S., Camy-Peyret, C., and Coheur, P. F.: Characterization of methane retrievals from the IASI space-borne sounder, Atmos. Chem. Phys., 9, 7889–7899, doi:10.5194/acp-9-7889-2009, 2009.
Remer, L. A., Kaufman, Y. J., Tanré, D., Mattoo, S., Chu, D. A., Martins, J. V., Li, R. R., Ichoku, C., Levy, R. C., Kleidman, R. G., Eck, T. F., Vermote, E., and Holben, B. N.: The MODIS Aerosol Algorithm, Products, and Validation, J. Atmos. Sci., 62, 947–973, 2005.
Rodgers, C. D.: Inverse Methods for Atmospheric Sounding: Theory and Practice, World Sci., Hackensack, NJ, 2000.
Rothman, L. S., Gordon, I. E., Barbe, A., Benner, D. Chris, Bernath, P. F., Birk, M., Boudon, V., Brown, L. R., Campargue, A., Champion, J.-P., Chance, K., Coudert, L. H., Dana, V., Devi, V. M., Fally, S., Flaud, J.-M., Gamache, R. R., Goldman, A., Jacquemart, D., Kleiner, I., Lacome, N., Lafferty, W. J., Mandin, J.-Y., Massie, S. T., Mikhailenko, S. N., Miller, C. E., Moazzen-Ahmadi, N., Naumenko, O. V., Nikitin, A. V., Orphal, J., Perevalov, V. I., Perrin, A., Predoi-Cross, A., Rinsland, C. P., Rotger, M., Šimečková, M., Smith, M. A. H., Sung, K., Tashkun, S. A., Tennyson, J., Toth, R. A., Vandaele, A. C., and Vander Auwera, J.: The HITRAN 2008 molecular spectroscopic database, J. Quant. Spectrosc. Ra., 110, 533–572, 2009.
Schlüssel, P., Hultberg, T. H., Phillips, P. L., August, T., and Calbet, X.: The operational IASI Level 2 processor, Adv. Space Res., 36, 982–988, 2005.

AMTD
5, 8435–8468, 2012

Scott N. A.: A direct method of computation of transmission function of an inhomogeneous gaseous medium: description of the method and influence of various factors, J. Quant. Spectrosc. Ra., 14, 691–707, 1974.

Shannon, C. E. and Weaver, W.: The Mathematical Theory of Communication, Univ. of Illinois Press, 1949.

Stamnes, K., Tsay, S., Wiscombe, W., and Jayaweera, K.: Numerically stable algorithm for discrete-ordinate-method radiative transfer in multiple scattering and emitting layered media, Appl. Opt. 27, 2502–2509, 1988.

Strow, L. L., Hannon, S. E., Weiler, M., Overoye, K., Gaiser, S. L., and Aumann, H. H.: Prelaunch spectral calibration of the atmospheric infrared sounder (AIRS), IEEE T. Geosci. Remote, 41, 274–286, 2003.

Sutherland, R. and Khanna, R.: Optical properties of organic based aerosols produced by burning vegetation, Aerosol Sci. Technol., 14, 331–342, 1991.

Tanré, D., Bréon, F. M., Deuzé, J. L., Dubovik, O., Ducos, F., Franàçois, P., Goloub, P., Herman, M., Lifermann, A., and Waquet, F.: Remote sensing of aerosols by using polarized, directional and spectral measurements within the A-Train: the PARASOL mission, Atmos. Meas. Tech., 4, 1383–1395, doi:10.5194/amt-4-1383-2011, 2011.

Tanré, D., Brogniez, C., Derimian, Y., Dubuisson, P., Goloub, P., Herbin, H., Mortier, A., Minvielle, F., Sauvage, B., and Waquet, F.: Physical and optical properties, composition and transport of the Eyjafyallajokull plume in April–May 2010, Atmos. Chem. Phys., in preparation, 2012.

Volz, F.: Infrared optical constants of ammonium sulfate, sahara dust; volcanic pumice and flyash, Appl. Opt., 12, 564–568, 1973.

Worden, J., Bowman, K., Noone, D., Beer, R., Clough, S., Eldering, A., Fisher, B., Goldman, A., Gunson, M., Herman, R., Kulawik, S. S., Lampel, M., Luo, M., Osterman, G., Rinsland, C., Rodgers, C., Sander, S., Shephard, M., and Worden, H.: Tropospheric Emission Spectrometer observations of the tropospheric HDO/H_2O ratio: Estimation approach and characterization, J. Geophys. Res., 111, D16309, doi:10.1029/2005JD006606, 2006.

Worden, J., Kulawik, S., Frankenberg, C., Payne, V., Bowman, K., Cady-Peirara, K., Wecht, K., Lee, J.-E., and Noone, D.: Profiles of CH_4, HDO, H_2O, and N_2O with improved lower tropospheric vertical resolution from Aura TES radiances, Atmos. Meas. Tech., 5, 397–411, doi:10.5194/amt-5-397-2012, 2012.

Xiong, X., Barnet, C., Maddy, E., Sweeney, C., Liu, X., Zhou, L., and Goldberg, M.: Characterization and validation of methane products from the Atmospheric Infrared Sounder (AIRS), J. Geophys. Res., 113, G00A01, doi:10.1029/2007JG000500, 2008.

Yoshida, Y., Ota, Y., Eguchi, N., Kikuchi, N., Nobuta, K., Tran, H., Morino, I., and Yokota, T.: Retrieval algorithm for CO_2 and CH_4 column abundances from short-wavelength infrared spectral observations by the Greenhouse gases observing satellite, Atmos. Meas. Tech., 4, 717–734, doi:10.5194/amt-4-717-2011, 2011.

AMTD
5, 8435–8468, 2012

Table 1. Summary of assumed aerosol parameters adapted from Dubovik et al., 2002; Tanré et al., 2012. C is number of particles in part m^{-3}, r is mean radius in µm, and σ is deviation of the radius in µm. The f and c indices are for fine and coarse mode respectively. $\tau_{(1020)}$, $\tau_{(865)}$, $\tau_{(440)}$, corresponds to the optical depth at 1020, 865 and 440 nm, respectively.

Aerosol type	C_f (part m^{-3})	r_f (µm)	ln(σ_f)	C_c (part m^{-3})	r_c (µm)	ln(σ_c)
Dust	$1.58\times10^9 + 7.92\times10^9\tau_{(1020)}$	0.088	0.42	$-7.8\times10^5 + 3.573\times10^7\tau_{(1020)}$	0.832	0.61
Biomass	$6.97\times10^7\tau_{(440)}/r_f^3$	$0.087 + 810^{-3}\tau_{(440)}$	0.40	$3.598\times10^5\tau_{(440)}/r_c^3$	$0.503 + 0.089\tau_{(440)}$	0.79
Ash	1.003×10^8	0.130	0.37	$3.287\times10^7\tau_{(865)}$	0.805	0.76

AMTD
5, 8435–8468, 2012

Multispectral information for gas and aerosol retrieval

H. Herbin et al.

Table 2. Gaseous columns total errors for assumed or retrieved aerosol parameters.

	H_2O	CO_2	CH_4
Ash fixed	0.88 %	1.67 %	2.96 %
Ash retrieved	0.82 %	1.48 %	2.66 %
Biomass fixed	1.38 %	0.82 %	2.42 %
Biomass retrieved	0.40 %	0.29 %	0.88 %
Dust fixed	1.39 %	2.90 %	2.75 %
Dust retrieved	0.56 %	0.52 %	1.10 %

AMTD
5, 8435–8468, 2012

AMTD
5, 8435–8468, 2012

Multispectral information for gas and aerosol retrieval

H. Herbin et al.

Table 3. Channels selected quantity (in %) from each band for simultaneous gas and aerosol retrieval.

	Band 4	Band 3	Band 2	Band 1
Ash	41.1 %	0.1 %	27.7%	31.1 %
Biomass	55.4 %	23.6 %	0.2 %	20.8 %
Dust	70.0 %	0.1 %	5.2 %	24.7 %

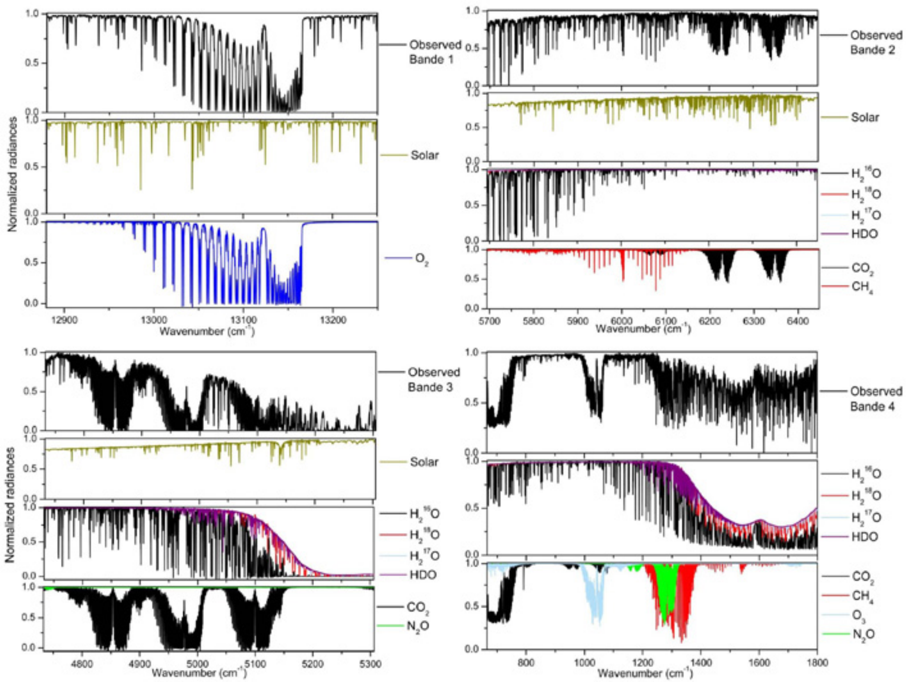

Fig. 1. Example of TANSO-FTS spectrum in normalized radiances, solar contribution and individual major molecular absorbers. Each band is calculated from our line-by-line forward model on US Standard profiles.

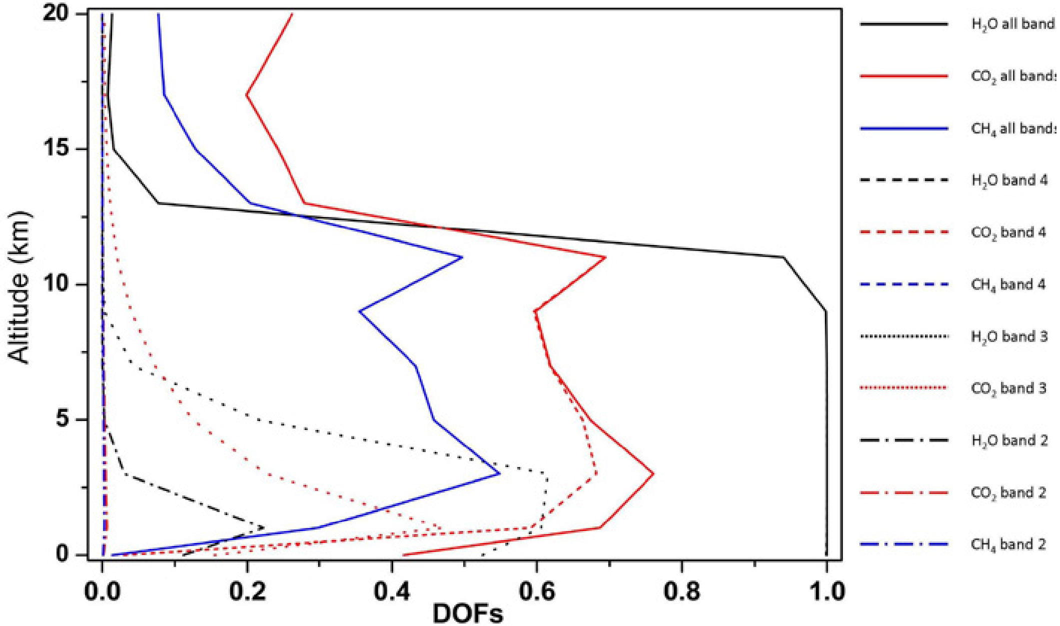

Fig. 2. DOFs of H_2O (black lines), CO_2 (red lines) and CH_4 (blue lines) vertical profiles for Bands 2 (dash and dot), 3 (dot), 4 (dash) separately and all the bands together (solid lines).

AMTD

5, 8435–8468, 2012

Multispectral information for gas and aerosol retrieval

H. Herbin et al.

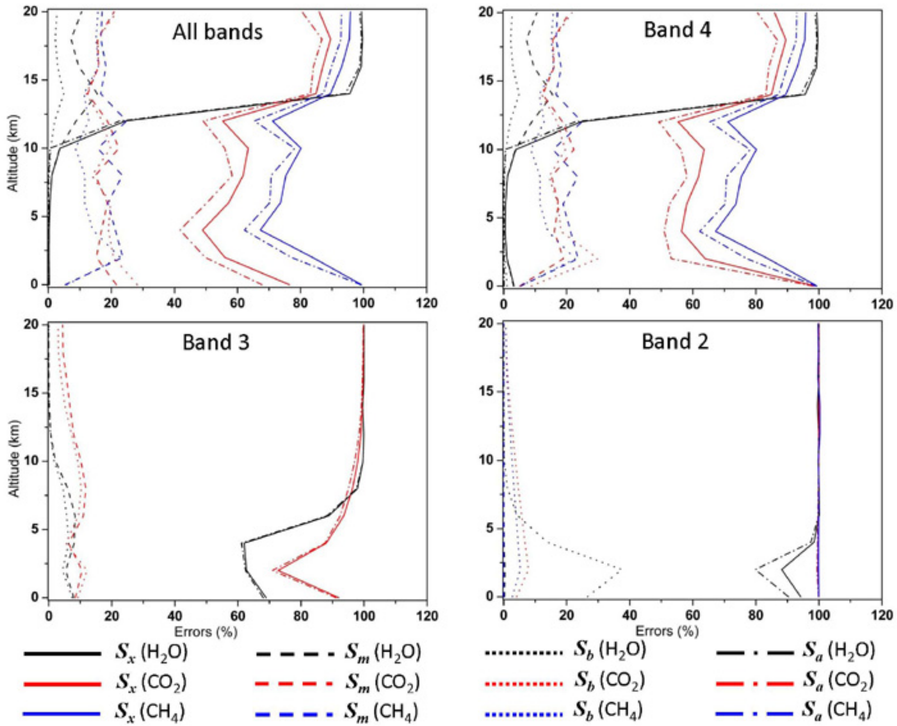

Fig. 3. Errors of H_2O (black lines), CO_2 (red lines) and CH_4 (blue lines) vertical profiles for Bands 2, 3, 4 separately and all the bands together. $\mathbf{S}_x$ (solid lines) denote the total error profiles; $\mathbf{S}_a$ (dash/dot), $\mathbf{S}_b$ (dot), and $\mathbf{S}_m$ (dash) correspond to the contributions of the a priori, non-retrieved parameters, and measurements errors respectively.

AMTD
5, 8435–8468, 2012

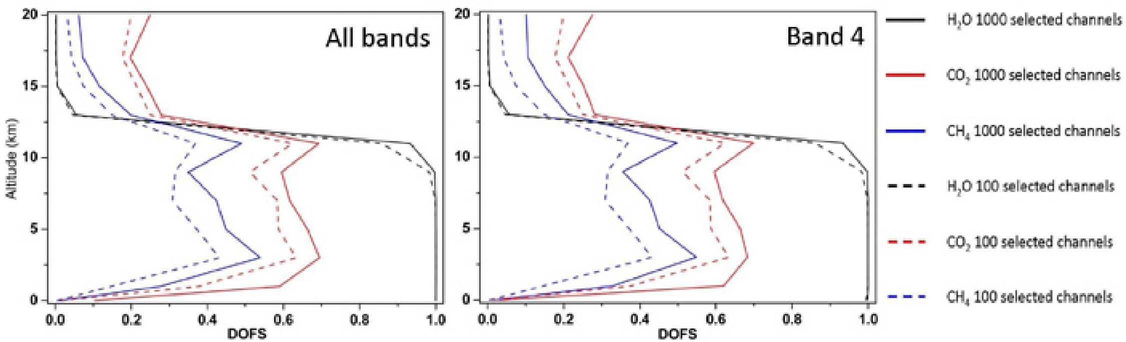

Fig. 4. DOFs of H_2O (black lines), CO_2 (red lines) and CH_4 (blue lines) vertical profiles for Band 4 (dash) and all the bands (solid line) in case of channels selection.

AMTD
5, 8435–8468, 2012

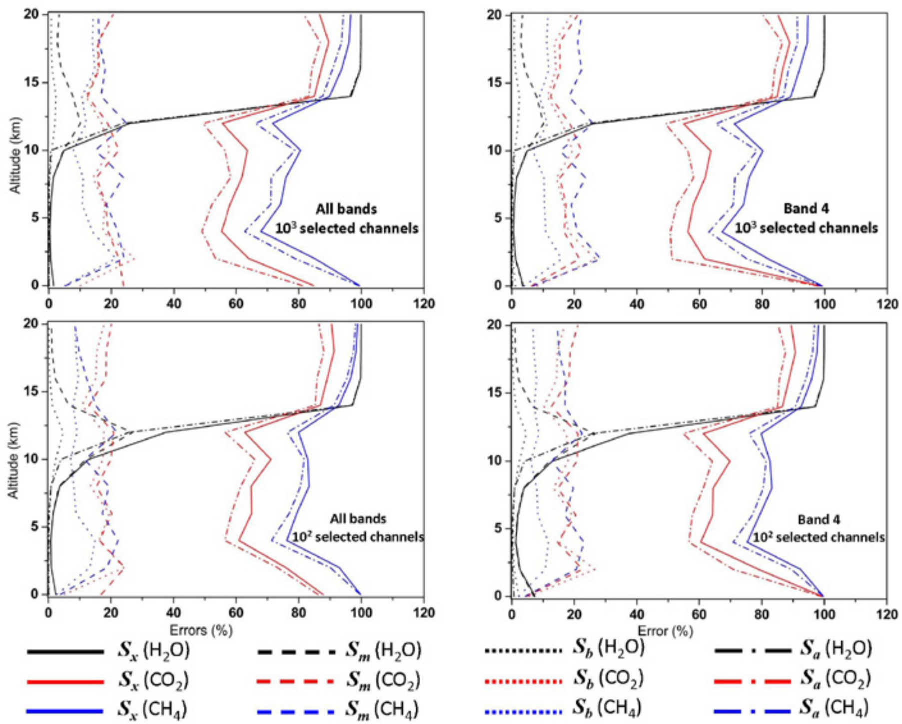

Fig. 5. Errors of H_2O (black lines), CO_2 (red lines) and CH_4 (blue lines) vertical profiles for Band 4 and all the bands in case of channels selection. $\mathbf{S}_x$ (solid lines) denote the total error profiles; $\mathbf{S}_a$ (dash/dot), $\mathbf{S}_b$ (dot), and $\mathbf{S}_m$ (dash) correspond to the contributions of the a priori, non-retrieved parameters, and measurements errors respectively.

AMTD
5, 8435–8468, 2012

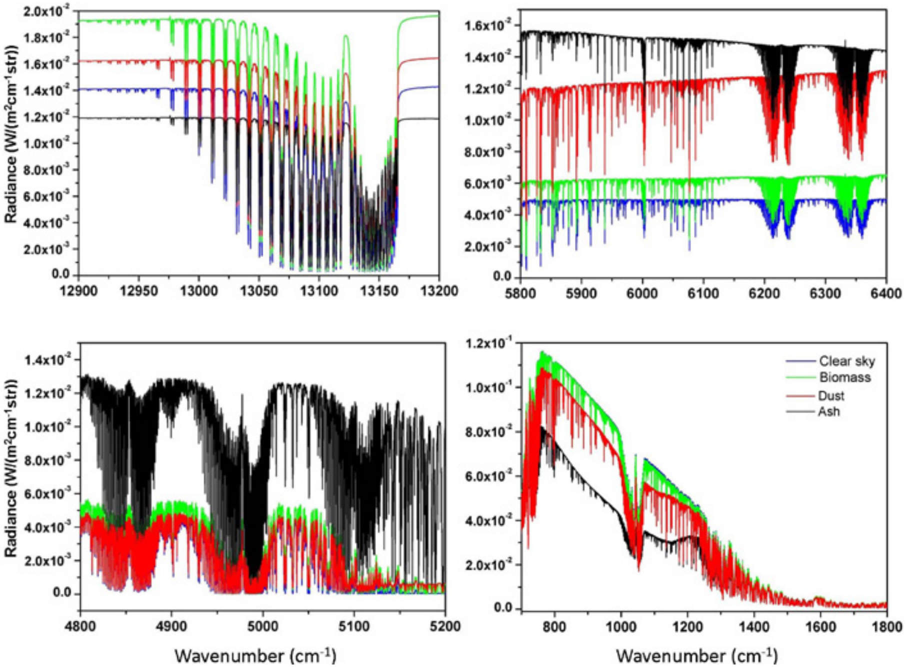

Fig. 6. Simulated TANSO-FTS spectra in radiances (W/(m^2 cm^{-1} str)) for clear sky condition (blue lines), in presence of volcanic ash (black lines) with an optical thickness $\tau_{(865\,\text{nm})} = 2.35$, biomass burning particles (green lines) with $\tau_{(440\,\text{nm})} = 0.75$, and dust (red lines) with $\tau_{(1020\,\text{nm})} = 0.25$.

AMTD
5, 8435–8468, 2012

Multispectral information for gas and aerosol retrieval

H. Herbin et al.

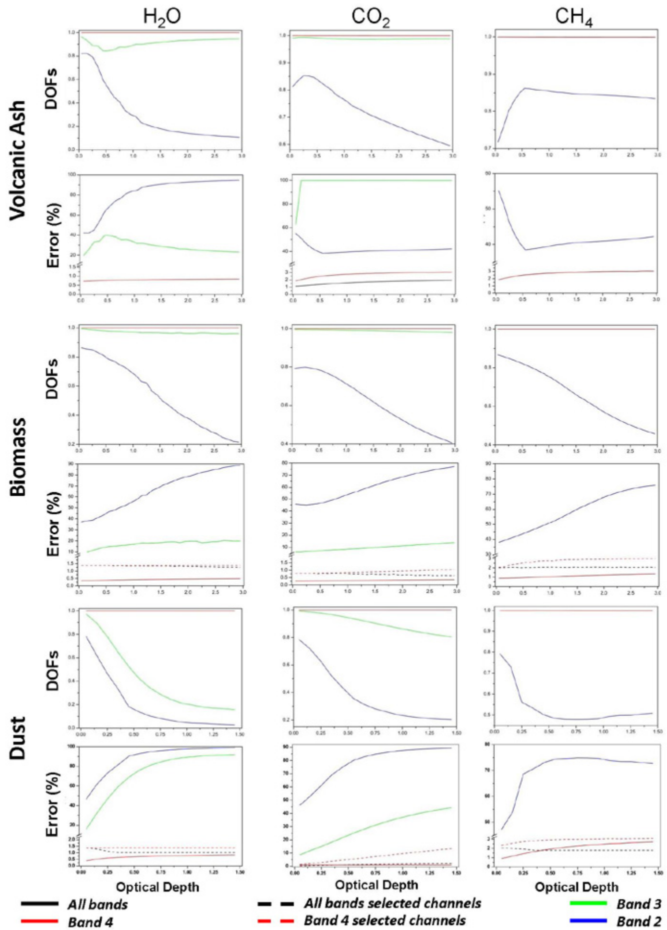

Fig. 7. Gaseous columns DOFs and errors (in %) vs. aerosol optical depth.

AMTD
5, 8435–8468, 2012

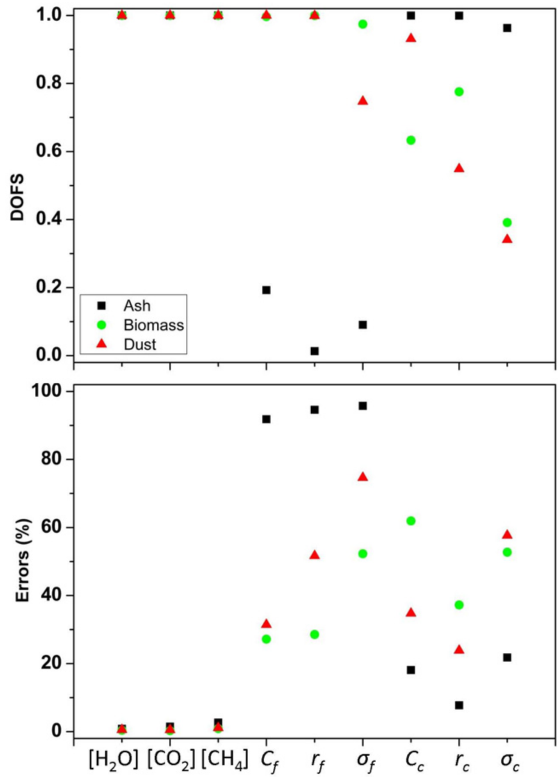

Fig. 8. DOFs (upper panel) and total error (in %, bottom panel) for each parameter of the state vector. The black squares are for volcanic ash, green circles are for biomass particles and red triangles are for dust. H_2O, CO_2, and CH_4 are for total columns of each gas; C is number of particles, r is mean radius and σ is deviation of the radius. The f and c indices are for fine and coarse mode respectively.

AMTD
5, 8435–8468, 2012